Applied Physics Letters

Observation and control of the anomalous Aharonov-Bohm oscillation in enhanced-mode topological insulator nanowire field-effect transistors

Cite as: Appl. Phys. Lett. **115**, 073107 (2019); https://doi.org/10.1063/1.5111180
Submitted: 24 May 2019 . Accepted: 18 July 2019 . Published Online: 14 August 2019

Hao Zhu, Curt A. Richter, Sheng Yu, Huixian Ye, Min Zeng, and Qiliang Li

Applied Physics Letters ARTICLE scitation.org/journal/apl

Observation and control of the anomalous Aharonov-Bohm oscillation in enhanced-mode topological insulator nanowire field-effect transistors

Cite as: Appl. Phys. Lett. **115**, 073107 (2019); doi: 10.1063/1.5111180
Submitted: 24 May 2019 · Accepted: 18 July 2019 ·
Published Online: 14 August 2019

Hao Zhu,[1,a)] Curt A. Richter,[2] Sheng Yu,[3] Huixian Ye,[3,4] Min Zeng,[4] and Qiliang Li[3,a)]

AFFILIATIONS

[1]State Key Laboratory of ASIC and System, School of Microelectronics, Fudan University, Shanghai 200433, China
[2]Engineering Physics Division, National Institute of Standards and Technology, Gaithersburg, Maryland 20878, USA
[3]Department of Electrical and Computer Engineering, George Mason University, Fairfax, Virginia 22030, USA
[4]Institute for Advanced Materials, South China Normal University, Guangzhou 510006, China

[a)]**Authors to whom correspondence should be addressed:** hao_zhu@fudan.edu.cn and qli6@gmu.edu

ABSTRACT

Aharonov-Bohm (AB) oscillation is a quantum mechanical phenomenon which reveals the coupling of electromagnetic potentials with the electron wave function, affecting the phase of the wave function. Such a quantum interference effect can be demonstrated through the magnetotransport measurement focusing on low-dimensional electronic states. Here, we report the experimental observation of anomalous AB oscillation in an enhanced-mode topological insulator Bi_2Se_3 nanowire field-effect transistor (FET) under strong surface disorder, which is different from the reported AB oscillation in topological insulator nanostructures. The surrounding gate of the nanowire FET gives rise to tunability of the chemical potential and introduces strong disorder on the surface states, leading to primary oscillation with an anomalous h/e period. Furthermore, the oscillation exhibits a significant dependence on the gate voltage which has been preliminary explained with the quantization of the surface conduction channel. The experimental demonstration can be very attractive for further exploration of quantum phase interference through electrical approaches, enabling applications in future information and electromagnetic sensing technology.

Topological insulators have drawn growing interest since the first discovery as a unique electronic state of matter with insulating bulk but gapless surface states.[1–4] The appealing applications of topological insulators in quantum information technology and condensed matter physics include the realization of the elusive Majorana fermions and the detection of magnetic monopoles, which, however, require strong and effective quantum control over the surface states.[5–7] The electronic surfaces have been observed and studied for many years,[8–10] but the discovery of three-dimensional topological insulators has facilitated the control and manipulation over the exotic electronic states. In conventional experimental research, such control was largely attempted by integrating topological insulators in various heterogeneous structures, highlighting the topological feature of the surface states via external stimuli such as light, magnetic field, and electric field. However, the traditional three-dimensional topological insulator will inevitably encounter the interference from the bulk conduction, and most external stimuli have intrinsic limitations restricting the manipulation on the surface states.

Recently, topological insulator nanostructured materials have attracted increasing attention due to their large surface-to-volume ratio and can therefore manifest the surface effects.[11–13] The protected conducting surface states are immune to time-reversal-invariant perturbations including crystal defects and nonmagnetic impurities which, on the contrary, can substantially impact the conduction of the bulk. In nanoscale topological insulator materials such as nanowires and nanoribbons where the quantum interference effects are more prominent with smaller sample size, the transport signatures of the bulk may diminish, shedding more light on the topological features of the robust surface states. A magnetotransport study on topological insulator nanostructures has been proved to be an effective approach to identify the surface states through the demonstration of quantum oscillations such as Shubnikov-de Haas (SdH)[11,14] oscillation and

Aharonov-Bohm (AB) interference.[15,16] By applying a magnetic field (B) along the length of the quasi-1D nanostructure, the quantum interference effects will be observed when the electrons on the topological insulator surface propagate in closed trajectories encircling a certain amount of magnetic flux (multiple of $^1/_2\Phi_0 = h/2e$, where h is Planck's constant and e is the electron charge). With the presence of strong disorder, even multiples of $^1/_2\Phi_0$ flux can lead to a fully localized state, while odd multiples of $^1/_2\Phi_0$ flux lead to a π AB phase, resulting in a metallic state, demonstrated by conductance maxima in the h/e oscillations.[15,17] Recent transport measurements on topological insulator nanoribbons have shown the AB interference with h/e oscillations.[18,19] However, the magnetoresistance was found at minimum in the h/e flux period AB oscillations in these reports. Although the observed AB effect is consistent with the strong spin–orbit coupling in the Bi_2Se_3 nanoribbon, such primary h/e oscillations and the secondary $h/2e$ oscillations are most likely arising from the weakly disordered regime, resembling the h/e and $h/2e$ oscillations in individual normal-metal rings. This is mostly due to the planar device geometry without effective and strong electrical gating, which can be expected to enhance the electric field across the topological insulator inducing strong surface disorder.

Here, we report the experimental observation of the anomalous AB effect with strong disorder on the surface from a high-performance gate-surrounding Bi_2Se_3 nanowire field-effect transistor (FET). We demonstrate that the pronounced oscillations have a period of h/e under strong surface disorder introduced by tuning the chemical potential through the surrounding top gate. The periodicity in the AB oscillation can be further adjusted through the quantization of the surface conduction channel. Such tuning of the quantum interference effects realized in the enhanced-mode Bi_2Se_3 nanowire FET has paved an attractive way for the use of quantum mechanics-related phenomena for future quantum computing and is very promising toward the design of quantum devices for applications in information and sensing technology.

The Bi_2Se_3 nanowires were grown in a low-pressure chemical vapor deposition (LPCVD) furnace following the catalytic vapor-liquid-solid (VLS) mechanism. In detail, a layer of 300 nm SiO_2 was first grown on a cleaned Si substrate by dry oxidation. Then, a thin film of the Au catalyst (2–3 nm) was deposited onto a patterned area predefined by photolithography. Next, the Bi_2Se_3 nanowires were grown from the catalyst at 540 °C for 2 h in a LPCVD tube furnace in a vacuum environment. The as-grown Bi_2Se_3 nanowires are typically 20 μm in length with a diameter range of 30 nm to150 nm. After the growth of Bi_2Se_3 nanowires, 3 nm/100 nm Ti/Pt source/drain (S/D) electrodes were directly patterned by photolithography and formed by electron beam evaporation and lift-off processes. The channel length was defined to be 4 μm. A layer of 30 nm HfO_2 was then deposited as the top-gate dielectric covering the nanowire channel at 250 °C by atomic layer deposition (ALD) with tetrakis(ethylmethylamino)hafnium (TEMAH) and water (H_2O) as precursors. A 100 nm Pd top gate was finally defined by photolithography and formed by similar electron beam evaporation and lift-off processes. The fabrication of the Bi_2Se_3 nanowire FET does not include any nanowire harvesting and aligning steps. As a result, simultaneous batch fabrication can be enabled using the reproducible and homogeneous CVD single-crystal nanowires with ultraclean interfaces.

The schematic of the Bi_2Se_3 nanowire FET and a transmission electron microscopy (TEM) image of the device cross section are shown in Figs. 1(a) and 1(b), respectively. The Bi_2Se_3 nanowire with a

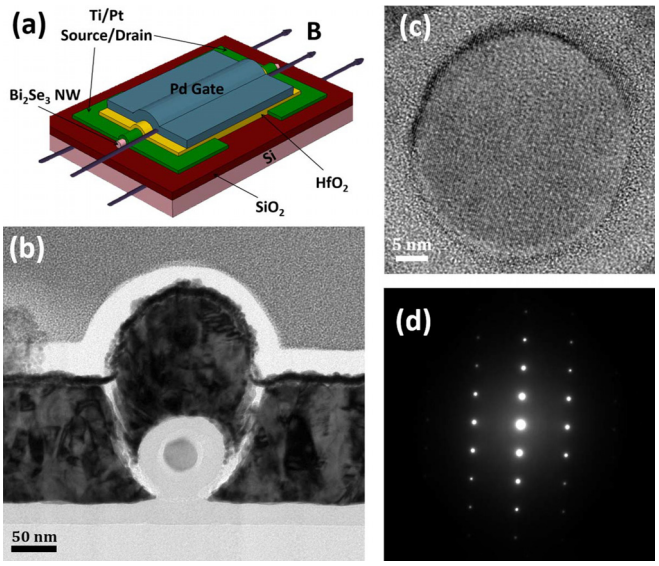

FIG. 1. (a) Schematic structure of a Bi_2Se_3 nanowire FET with an external magnetic field applied along the channel direction. (b) TEM image of the cross section of the Bi_2Se_3 nanowire FET. HRTEM images of the Bi_2Se_3 nanowire (c) focusing on the nanowire channel and (d) showing the single-crystal rhombohedral phase.

diameter of ~40 nm was surrounded by the HfO_2 layer and the Omega-shaped top gate. The high-resolution TEM (HRTEM) image shown in Figs. 1(c) and 1(d) demonstrates that the Bi_2Se_3 nanowire is a high-quality single crystal with a well-defined rhombohedral structure. We first measured the drain current (I_{DS}) vs top gate voltage (V_{GS}) transfer characteristics at 4 K under a magnetic field parallel to the nanowire channel with different intensities [the B field direction indicated in Fig. 1(a)]. As reported in our previous work, our surrounding gate enabling excellent electrostatic control over the nanowire channel can deplete the electrons both in the bulk and on the surface.[20] As a result, although the bandgap of most chalcogenide topological insulators is quite small (e.g., 0.35 eV for Bi_2Se_3), the fabricated FET device can still exhibit good switching behaviors at low temperature. As shown in Fig. 2(a), clear cutoff current and sharp turn-on have been obtained [I_{DS}-V_{GS} curves on a linear scale shown in the inset of Fig. 2(a)]. No shift in threshold voltage (V_{TH}) or change in subthreshold swing (SS) was observed by changing the magnetic field intensity from the I_{DS}-V_{GS} curves. This indicates that the influence of dielectric interface states is negligible, and the capacitance between the nanowire channel and the ground has no magnetic field dependence. The output characteristics are shown in Fig. 2(b) with smooth and well-saturated I_{DS} vs V_{DS} (V_{DS}: drain-source voltage) curves, suggesting an enhanced-mode transistor.

With such high-performance Bi_2Se_3 nanowire FETs, we focus on the quantum interference effect by probing the magnetotransport properties under an external magnetic field applied parallel to the nanowire channel. The conduction electrons on the surface states propagate along the perimeter of the nanowire which has a larger surface-to-volume ratio than the bulk material, demonstrating the well-known AB effect in the low-temperature transport properties. As illustrated in Fig. 2(c), upon the application of a certain V_{GS} (2.9 V) switching the

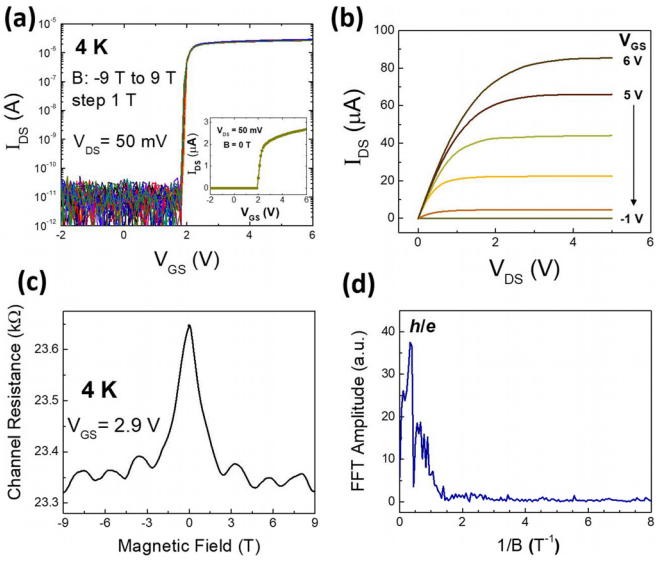

FIG. 2. (a) Transfer characteristics (I_{DS}-V_{GS}) of the Bi_2Se_3 nanowire FET at various magnetic field intensities ranging from −9 T to 9 T. V_{DS} was maintained at 50 mV. Inset: The linear-scale transfer characteristics. (b) Output characteristics (I_{DS}-V_{DS}) of the Bi_2Se_3 nanowire FET under different V_{GS}. (c) Oscillatory features of the magnetoresistance obtained by sweeping the magnetic field between ±9 T. (d) FFT analysis showing the amplitude as a function of 1/B. The location of *h*/*e* was labeled.

FET to on state, a pronounced AB oscillation in magnetoresistance has been observed when sweeping the magnetic field between ±9 T. A sharp localization peak at zero field is seen, and an average oscillation period of 2.23 T is obtained. For the *h*/*e* AB interference effect, such a period corresponds to a cross-sectional area of 1.85×10^{-15} m^2 [about 48 nm in diameter by assuming a cylindrical nanowire channel, at the same level as the TEM results shown in Fig. 1] according to the AB effect which describes the oscillation period as $\Delta B = \Phi_0/A$, where A is the cross-sectional area of the Bi_2Se_3 nanowire.[21,22] The discrepancy between these two values can be attributed to the change in the magnetic flux encircled by the electrons through the nanowire cross section due to the strong surrounding-gate control and the coupling between the gate electric field and external magnetic field, which will be explained later in the paper. A fast Fourier transform (FFT) was performed to better understand the origin of the AB oscillations. As shown in Fig. 2(d), prominent *h*/*e* oscillation has been clearly observed. It is a direct evidence of the interference effect, indicating that the carriers travel through the full perimeter of the nanowire. This is in agreement with the reported scenario of topological insulator nanoribbons in larger size, where the electrons not only exist on the top and bottom surfaces but also propagate on the two side walls.[18,19] However, it is worth to mention that the smaller aspect ratio in these nanoribbons (e.g., 350 nm circumference and 2 μm length in Ref. 18 and 430 nm circumference and 2 μm length in Ref. 19) can lead to a very long localization length of the system, contributing to antilocalization features and subsequent oscillations. In contrast, with the nanowires with a larger aspect ratio shown here (145 nm circumference and 4 μm length), it is easier to achieve strong surface disorder with a much shorter localization length, resulting in the time-reversal symmetry breaking by the magnetic field.

According to the theoretical study and numerical simulation, with odd multiples of *h*/2*e* flux, there is an additional Berry's phase of π on circling the cylindrical surface of a topological insulator, due to the surface curvature formed by the odd flux with the simplest illustration of a single Dirac cone.[13,17,23] Due to this Berry's phase, the conductance oscillation amplitude (note that we show the oscillation in magnetoresistance) will be approaching the ideal conductance (e^2/h) with odd flux through the nanowire. However, the situation will be different with different disorder strengths. With weak surface disorder where a large density of states is present, an antilocalization feature will be prominent contributing to an Altshuler-Aronov-Spivak (AAS) oscillation in magnetoconductance with the *h*/2*e* period and maximum at zero flux. We believe that is what Refs. 18 and 19 observed in their experiment in addition to the AB oscillations with the *h*/*e* flux period. The other amount of flux that does not break time-reversal symmetry in addition to the zero flux described above is of the value $^1/_2\Phi_0$, which can be interpreted with a phase of $2\pi\Phi/\Phi_0 = \pi$.[15] In our nanowire FETs, the top gate is used to effectively tune the Fermi level and reduce the bulk conductance contribution. The chemical potential is taken close to the Dirac point. In such strong disorder where the electron motion is near-ballistic, the phase shifting from 0 to π due to the spin of electrons is confined to the tangent plane to the circled surface and that is where the Berry's phase of π is introduced when completing the closed circle trajectories.[15,23] Our nanowire with a higher aspect ratio is thus in the localized regime with the magnetoresistance exhibiting maximum at zero flux as shown in Fig. 2(c).

We also characterized the AB oscillations when the Bi_2Se_3 nanowire FET was working in different regions by tuning gate bias. However, no oscillatory behavior was observed for the off state, and diminished oscillations with only clear zero-field localization peaks were observed for the subthreshold region (Figs. S1 and S2, supplementary material). As extracted from Fig. 2(a), the threshold voltage of the Bi_2Se_3 nanowire FET is around 2 V. Therefore, any applied gate voltage equals to or below 2 V will not turn on the FET. As discovered in our previous work, the charge carriers are fully depleted in the nanowire channel and only bulk conduction can be observed at higher temperatures by thermal excitation when V_{GS} is below V_{TH}.[20] With increasing gate voltage over V_{TH} but smaller conduction current as compared with the on state (i.e., $\sim 2\,V < V_{GS} < \sim 2.8\,V$), the bulk conduction will be comparable to the surface conduction. The contribution from the bulk will destroy the phase coherence by scattering and the electrons' trajectories on the curved surface, leading to unclear oscillations. On the contrary, clear oscillatory features were obtained only at gate biases within a small range around 3 V as shown in Fig. 3, indicating that the electrons on the surface propagate along the perimeter of the nanowire with a phase π in the strong disordered system as discussed previously, leading to a metallic state. It is in agreement with our previous results that the on-state current is linear to the over threshold voltage, and this metallic conduction is most likely flowing at the surface.[20] A sudden drop has been observed in the magnetoresistance at a higher B field (beyond ±8 T), and such drop is more obvious at higher gate voltage. We attribute it to the magnetoresistance background which is typically parabolic in R vs B curves. With increasing gate voltage, the amount of charges on the surface will increase significantly. Meanwhile, the number of trivial carriers in the bulk will also increase blurring of the surface conduction-based AB oscillatory features. Thus, the parabolic background will be highlighted.

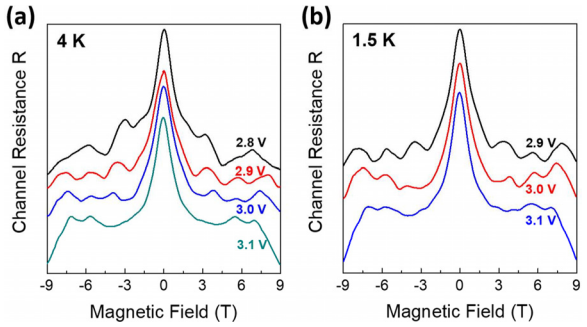

FIG. 3. (a) Magnetoresistance as a function of the magnetic field at 4 K under four different V_{GS}. (b) Magnetoresistance as a function of the magnetic field at 1.5 K under three different V_{GS}. The curves have been vertically shifted for better illustration. The plots without curve shifting are shown in Fig. S3 (supplementary material).

We then further compared the magnetoresistance oscillations under different gate voltages by plotting the oscillation period (ΔB) extracted from Fig. 3 as a function of V_{GS}. As shown in Fig. 4(a), it is interesting to find a clear decrease in the oscillation period. By assuming that the density of magnetic flux encircled by the trajectories of conduction electrons remains constant under the external magnetic field with fixed intensity, the decreasing trend in the oscillation period indicates the enlargement of the effective cross-sectional area of the nanowire channel under increasing gate voltage. It can be easily inclined to attribute this phenomenon to the shifting of inversion layer charge centroid toward the Bi_2Se_3/HfO_2 interface with the presence of a stronger electric field induced by higher gate voltage. Different from the conventional charge/current model, the quantum confinement effect is remarkable in nanoscale nanowire FETs with enhanced gate control and is indispensable to be considered under the inversion condition as the electron energies are quantized occupying discrete energy levels.[24,25] Various charge centroid models incorporating the quantum effects have been reported.[26–29] Here, we borrow the modified charge/current model based on the cylindrical surrounding-gate transistor by Roldán *et al.* giving the inversion charge centroid as[29]

$$\frac{1}{t_{inv}} = \frac{1}{a+2bR} + \frac{1}{t_{inv0}}\left(\frac{N_{inv}}{N_{inv0}(R)}\right)^{n}, \tag{1}$$

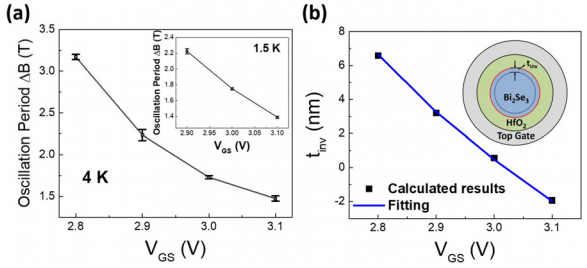

FIG. 4. (a) The oscillation period ΔB as a function of gate voltage at 4 K. Inset: ΔB vs V_{GS} at 1.5 K. The error bars were marked by calculating the oscillation period for four times. (b) Calculation (black dots) and fitting (blue line) results of the inversion layer thickness. Inset: Schematic of the cross section of the Bi_2Se_3 nanowire FET showing the inversion layer thickness.

where t_{inv} is the inversion layer thickness [indicated in the inset of Fig. 4(b)], N_{inv} is the electron density per unit area, R is the nanowire radius, and a, b, t_{inv0}, and n are constants not dependent on the gate bias. Note that $N_{inv} = Q_{inv}/2\pi Rq$ is V_{GS}-depended since Q_{inv} is proportional to $(V_{GS}-V_{TH})$. We first calculated the effective radius formed by the inversion charge carriers encircling the magnetic flux under different V_{GS} (see the supplementary material for details). As shown in Fig. 4(b) (black square dots), t_{inv} decreases with higher V_{GS} (more inversion charge), which agrees with expectation since the charge distribution shifts toward the Bi_2Se_3/HfO_2 interface. Applying the model described by Eq. (1) on the nanowire FET, a perfect fitting has been observed, as demonstrated in Fig. 4(b) (blue line). It is worth mentioning here that the calculated t_{inv} at 3.1 V V_{GS} is negative which is due to the fact that only the inversion layer quantization effect was considered. Further analysis incorporating other mechanisms describing the electromagnetic coupling between the electric field and the external magnetic field will shed more light on the phenomenon reported here. For example, such coupling has been theoretically confirmed and is known as the topological magnetoelectric (TME) effect. The TME effect describes the electromagnetic response of the topological insulator under a strong electric field. In our nanowire FET, the total magnetic flux encircled by the electrons can be changed by the induced magnetization originated from the superposition of the gate electric field and the electric field between the source and drain. This also explains the difference in the nanowire diameter between the TEM results and the calculation. Although this is only our preliminary assumption and needs further investigation, the fitting result by using the charge centroid model perfectly matches the calculated values, suggesting the necessity to include the inversion layer quantization effect in the analysis of changes in the AB oscillation period and the gate voltage tuning of the oscillation in nanoscale topological insulator FETs.

In summary, we have integrated a Bi_2Se_3 topological insulator nanowire in a high-performance enhanced-mode FET device platform and observed anomalous AB oscillation. The strongly disordered surface states of the nanowire have led to the primary AB oscillation, indicating carrier propagation along the nanowire surface perimeter. The oscillation period exhibits a dependence on a small gate voltage, enabling tenability by the surface conduction channel quantization. Our study has provided excellent basis for a further study on the electromagnetic coupling between the electric field and the magnetic field. It is promising to achieve effective control over the quantum interference effects by using electrically accessible approaches. This can pave a robust pathway for future quantum information and sensing technology.

See the supplementary material for the details of calculation of the inversion layer thickness, the magnetoresistance oscillations with the FET operating in other regions at 4 K and 1.5 K, the gate voltage dependence of the AB oscillation without curve shifting, and the schematic setup for the magnetotransport measurement.

Q.L. acknowledges the support from the National Science Foundation under Grant No. ECCS-1809399. H.Z. acknowledges the financial support from the Shanghai Pujiang Program under Grant No. 17PJ1400500. We acknowledge the discussions with L.-I. Huang and Y. Fukuyama and the support from D. B. Newell for the magnetotransport

measurement. We thank the Center for Nanoscale Science and Technology at the NIST for device fabrication technical support.

REFERENCES

[1]M. Z. Hasan and C. L. Kane, "Colloquium: topological insulators," Rev. Mod. Phys. **82**, 3045–3067 (2010).
[2]Y. Li, X. Zhou, and C. Wu, "Two- and three-dimensional topological insulators with isotropic and parity-breaking Landau levels," Phys. Rev. B **85**, 125122 (2012).
[3]D. Wang, S. Xu, Y. Wang, and C. Wu, "Detecting edge degeneracy in interacting topological insulators through entanglement entropy," Phys. Rev. B **91**, 115118 (2015).
[4]T. Zhang, P. Cheng, X. Chen, J.-F. Jia, X. Ma, K. He, L. Wang, H. Zhang, X. Dai, Z. Fang, X. Xie, and Q.-K. Xue, "Experimental demonstration of topological surface states protected by time-reversal symmetry," Phys. Rev. Lett. **103**, 266803 (2009).
[5]D. Wang, Z. Huang, and C. Wu, "Fate and remnants of Majorana zero modes in a quantum wire array," Phys. Rev. B **89**, 174510 (2014).
[6]S. Cho, B. Dellabetta, A. Yang, J. Schneeloch, Z. Xu, T. Valla, G. Gu, M. J. Gilbert, and N. Mason, "Symmetry protected Josephson supercurrents in three-dimensional topological insulators," Nat. Commun. **4**, 1689 (2013).
[7]Y. Li, D. Wang, and C. Wu, "Spontaneous breaking of time-reversal symmetry in the orbital channel for the boundary Majorana flat bands," New J. Phys. **15**, 085002 (2013).
[8]I. Tamm, "On the possible bound states of electrons on a crystal surface," Phys. Z. Sowjetunion **1**, 733 (1932).
[9]E. Aerts, "Surface states of one-dimensional crystals (I)," Physcia **26**, 1047 (1960).
[10]H. Ohno, E. E. Mendez, J. A. Brum, J. M. Hong, F. Agulló-Rueda, L. L. Chang, and L. Esaki, "Observation of "Tamm states" in superlattices," Phys. Rev. Lett. **64**, 2555 (1990).
[11]Y. Yan, Z.-M. Liao, Y.-B. Zhou, H.-C. Wu, Y.-Q. Bie, J.-J. Chen, J. Meng, X.-S. Wu, and D.-P. Yu, "Synthesis and quantum transport properties of Bi_2Se_3 topological insulator nanostructures," Sci. Rep. **3**, 1264 (2013).
[12]J. J. Cha, K. J. Koski, and Y. Cui, "Topological insulator nanostructures," Phys. Status Solidi RRL **7**, 15–25 (2013).
[13]S. Cho, R. Zhong, J. A. Schneeloch, G. Gu, and N. Mason, "Kondo-like zero-bias conductance anomaly in a three-dimensional topological insulator nanowire," Sci. Rep. **6**, 21767 (2016).
[14]B. Sacépé, J. B. Oostinga, J. Li, A. Ubaldini, N. J. G. Couto, E. Giannini, and A. F. Morpurgo, "Gate-tuned normal and superconducting transport at the surface of a topological insulator," Nat. Commun. **2**, 575 (2011).
[15]J. H. Bardarson, P. W. Brouwer, and J. E. Moore, "Aharonov–Bohm oscillations in disordered topological insulator nanowires," Phys. Rev. Lett. **105**, 156803 (2010).
[16]S. Cho, B. Dellabetta, R. Zhong, J. Schneeloch, T. Liu, G. Gu, M. J. Gilbert, and N. Mason, "Aharonov–Bohm oscillations in a quasi-ballistic three-dimensional topological insulator nanowire," Nat. Commun. **6**, 7634 (2015).
[17]Y. Zhang and A. Vishwanath, "Anomalous Aharonov-Bohm conductance oscillations from topological insulator surface states," Phys. Rev. Lett. **105**, 206601 (2010).
[18]H. Peng, K. Lai, D. Kong, S. Meister, Y. Chen, X.-L. Qi, S.-C. Zhang, Z.-X. Shen, and Y. Cui, "Aharonov–Bohm interference in topological insulator nanoribbons," Nat. Mater. **9**, 225–229 (2010).
[19]F. Xiu, L. He, Y. Wang, L. Cheng, L.-T. Chang, M. Lang, G. Huang, X. Kou, Y. Zhou, X. Jiang, Z. Chen, J. Zou, A. Shailos, and K. L. Wang, "Manipulating surface states in topological insulator nanoribbons," Nat. Nanotech. **6**, 216–221 (2011).
[20]H. Zhu, C. A. Richter, E. Zhao, J. E. Bonevich, W. A. Kimes, H.-J. Jang, H. Yuan, H. Li, A. Arab, O. Kirillov, J. E. Maslar, D. E. Ioannou, and Q. Li, "Topological insulator Bi_2Se_3 nanowire high performance field-effect transistors," Sci. Rep. **3**, 1757 (2013).
[21]Y. Aharonov and D. Bohm, "Significance of electromagnetic potentials in the quantum theory," Phys. Rev. **115**, 485–491 (1959).
[22]T. Shen, Y. Q. Wu, M. A. Capano, L. P. Rokhinson, L. W. Engel, and P. D. Ye, "Magnetoconductance oscillations in graphene antidot arrays," Appl. Phys. Lett. **93**, 122102 (2008).
[23]Y. Zhang, Y. Ran, and A. Vishwanath, "Topological insulators in three dimensions from spontaneous symmetry breaking," Phys. Rev. B **79**, 245331 (2009).
[24]X. Baie and J. P. Colinge, "Two-dimensional confinement effects in gate-all-around (GAA) MOSFETs," Solid State Electron. **42**, 499–504 (1998).
[25]J. P. Colinge, X. Baie, and V. Bayot, "Evidence of two-dimensional carrier confinement in thin n-channel SOI gate-all-around (GAA) devices," IEEE Electron Device Lett. **15**, 193–195 (1994).
[26]Y.-C. King, H. Fujioka, S. Kamohara, W.-C. Lee, and C. Hu, "AC charge centroid model for quantization of inversion layer in n-MOSFET," in Proceeding of the Technical Papers, International Symposium on VLSI Technology, Systems, and Applications (1997), pp. 245–249.
[27]L. Ge and J. G. Fossum, "Analytical modeling of quantization and volume inversion in thin Si-film DG MOSFETs," IEEE Trans. Electron Dev. **49**, 287–294 (2002).
[28]J. J. Gu, H. Wu, Y. Liu, A. T. Neal, R. G. Gordon, and P. D. Ye, "Size-dependent-transport study of $In_{0.53}Ga_{0.47}As$ gate-all-around nanowire MOSFETs: Impact of quantum confinement and volume inversion," IEEE Electron Device Lett. **33**, 967–969 (2012).
[29]J. B. Roldán, A. Godoy, F. Gámiz, and M. Balaguer, "Modeling the centroid and the inversion charge in cylindrical surrounding gate MOSFETs, including quantum effects," IEEE Trans. Electron Dev. **55**, 411–416 (2008).